Average Flow Model of Rough Surface Lubrication: Flow Factors for Sinusoidal Surfaces

Nicolas Letalleur, Franck Plouraboué, Marc Prat

Average Flow Model of Rough Surface Lubrication: Flow Factors for Sinusoidal Surfaces

N. Letalleur

F. Plouraboué

M. Prat

Institut de Mécanique des Fluides de Toulouse,
UMR CNRS/INPT/UPS no. 5502,
Allée du Pr C. Soula 31400 Toulouse, France

The effects of lubricant film flow, pressurized and sheared between two parallel sinusoidal wavy surfaces in sliding motion is studied analytically. Results are presented using a flow factor model which provides an average description of the surfaces roughness impact. Two distinct cases are studied in order to compare stationary or time dependent local aperture configurations. Flow factors are computed respectively for each case through spatial or spatio-temporal average, revealing striking differences. The results shed light on the relevance of the composite roughness concept. Special attention is paid to the flow factor analytical behavior when surfaces are near contact. [DOI: 10.1115/1.1467084]

1 Introduction

The impact of surface roughness on lubrication is an important problem for many applications, albeit quite a difficult one. From a geometrical point of view only, it requires the computation of the flow over a time dependent fluid domain resulting from the motion and deformation of the moving solid surfaces. The more complex the surface (e.g., random, multi scaled, tridimensional roughness), the more difficult it is to understand the interplay between the surfaces topography and the observed macroscopic pressure, flux, and shear. Additional physical effects, such as cavitation, piezoviscosity or compressibility, among others, may contribute to the complexity of the problem but will be ignored in the analysis since, for simplicity, as far as up-scaling is concerned, they are generally discarded [1,2].

There is nevertheless an important body of literature that have been interested in such up-scaling description of sliding surfaces lubrication since the first developments of Christensen [3] and Chow et Cheng [4]. Different techniques have been used to derive macroscopic equations coupling the macroscopic flux, pressure and shear stress, with some ''flow factors'' that are related to the underlying surfaces geometry. Patir and Cheng [1,2] were the first to propose a heuristic model for general roughness patterns. Tripp [5] derived the correct tensorial form of the average flow model using a stochastic approach, while Bayada et al. [6,7] addressed the problem within the framework of the homogenization theory for spatially periodic structures and more recently volume averaging techniques [8] were used for macroscopisation of the flow between lubricated sliding surfaces with solid contacts [9].

The literature thus provides some averaged macroscopic model for lubricated sliding surfaces propounding a systematic method for the flow factors computation. The latter reference [9] has nevertheless pointed out that flow factors must be computed combining spatial and time average when the two surfaces are intercorrelated. Such correlation between solid surfaces occurs naturally during rolling process where roughness is transferred from the steel roll to the workpiece [10] as well as in any process where deformations conform the two pieces one another.

In the present paper, this precise issue is further analyzed considering a specific geometry for the sliding surfaces. Simple unidirectional sinusoidal wavy surface (Fig. 1) are chosen for careful investigation. Such one-dimensional anisotropic surface roughness, are relevant, in the context of laminating processes [10] or in those of magnetic recording disk [11–13] where surfaces presenting one-dimensional like streaks are commonly found.

This problem is of interest from at least four points of view: (1) it is, to a great extent, amenable to analytical developments, and thus it could be interesting to estimate the impact of some coarse description of surface roughness on flux, pressure and shear without any numerical computations, (2) the flow factor behaviors near contact can be obtained analytically, (3) the obtained results can be useful for testing numerical computation procedures, in particular for close contact lubrication studies, for which we give an explicit analytical treatment (4) it sheds light on the influence of inter-correlation between surfaces. In particular, we show that the concept of composite roughness does not apply where two surfaces are inter-correlated. Obviously, considering sinusoidal roughness as model roughness is not a novelty in the lubrication literature, [14–18]. However, to the best of our knowledge, the complete hereby presented analytical developments have not been reported previously.

As in [9] and [19], the analysis is restricted to non-deformable surfaces, isoviscous Newtonian and incompressible fluids. Cavitation, if any, is ignored as well as temperature variations. The local slopes being small, the flow at the roughness scale is described by the Reynolds (lubrication) equation. The flow is generated by the relative surfaces motion and the macroscopic pressure gradient.

2 Geometry and Kinematics

Figure 1 illustrates the geometry of the problem. y (resp. x) is the coordinate associated with (resp. perpendicular to) the streak direction. The top surface—defined as surface number 2—is moving at velocity $\mathbf{U}_2$ and the bottom one (surface 1) at velocity $\mathbf{U}_1$. Note that $\mathbf{U}_2$ and $\mathbf{U}_1$ are not necessarily collinear, and that there have zero vertical components. The characteristic wavelength λ of sinusoidal surfaces is the same on each surface. The surface amplitude is noted a and b respectively for surfaces 1 and 2. h is the local aperture and h_m is the mean distance between the two sur-

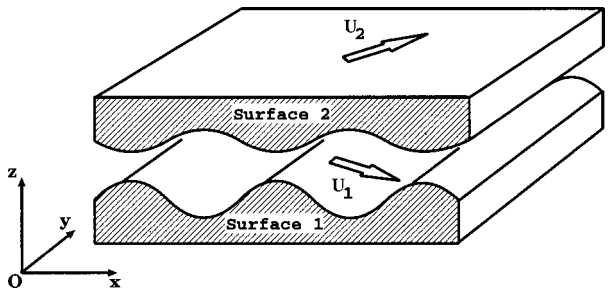

Fig. 1 Sketch of the situation studied

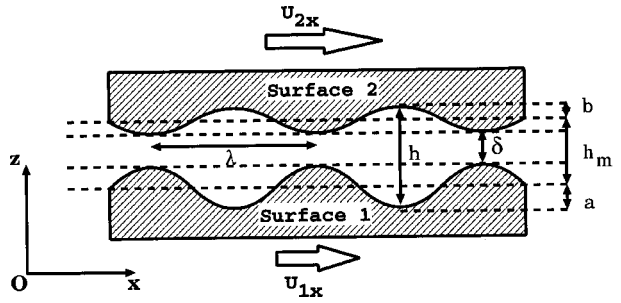

Fig. 2 Geometry in the plane $y=0$

faces. h_m can be defined as $h_m = a + b + \delta$ where δ is the minimum local aperture between the two surfaces (Fig. 2). In order to study the flow factor behaviors near contact, we define the dimensionless variable ϵ as $\epsilon = \delta/\sigma$ where σ is the composite r.m.s roughness classically defined as $\sigma = \sqrt{\sigma_1^2 + \sigma_2^2}$ (where σ_1 and σ_2 are the r.m.s roughness of each surface, which gives here $\sigma_1^2 = a^2/2$ and $\sigma_2^2 = b^2/2$). When surfaces touch one another, then $\epsilon = 0$ (i.e., $h_m = a + b$). In this limit, permanent contact occurs only when one of the two amplitudes a or b is zero. The time and space evolutions of surfaces height h_i, $i = 1,2$, are given by

$$h_i(x,t) = h_{io} + \sqrt{2}\sigma_i \sin\left(\frac{2\pi}{\lambda}(x - U_{ix}t) + \varphi_i\right)$$

where h_{io} is the mean planes of surfaces i related to the distance between both surfaces mean plane $h_m = h_{2o} - h_{1o}$, and φ_i is the surface phase at initial time t_o. The aperture field $h(x,t)$ then reads

$$h(x,t) = h_m + b\sin\left(\frac{2\pi}{\lambda}(x - U_{2x}t) + \varphi_2\right) - a\sin\left(\frac{2\pi}{\lambda}(x - U_{1x}t) + \varphi_1\right)$$

Defining the following dimensionless quantities:

$$H_\epsilon(X,t) = \frac{h(x,t)}{h_m}; \quad X = \frac{2\pi x}{\lambda}; \qquad A_\epsilon = \frac{a}{h_m} = \frac{a}{a+b+\epsilon\sigma}; \quad B_\epsilon = \frac{b}{h_m} \tag{1}$$

leads to express the local aperture in dimensionless form as

$$H_\epsilon(X,t) = 1 + B_\epsilon \sin(X - \omega_2 t + \varphi_2) - A_\epsilon \sin(X - \omega_1 t + \varphi_1) \tag{2}$$

where surface $i = 1,2$ pulsations are given by $\omega_i = 2\pi U_{ix}/\lambda$. According to Eq. (2), $H_\epsilon(X,t)$ can be regarded as the sum of two harmonic oscillators of pulsation ω_1 and ω_2, respectively. Classical developments (Appendix A) lead to express $H_\epsilon(X,t)$ as

$$H_\epsilon(X,t) = 1 + C_\epsilon(t)\sin(X + \theta_\epsilon(t)) \tag{3}$$

with

$$C_\epsilon(t) = \sqrt{A_\epsilon^2 + B_\epsilon^2 - 2A_\epsilon B_\epsilon \cos[(\omega_1 - \omega_2)t + \varphi_2 - \varphi_1]} \tag{4}$$

and

$$\theta_\epsilon(t) = \arctan\left[\frac{B_\epsilon \sin(\varphi_2 - \omega_2 t) - A_\epsilon \sin(\varphi_1 - \omega_1 t)}{B_\epsilon \cos(\varphi_2 - \omega_2 t) - A_\epsilon \cos(\varphi_1 - \omega_1 t)}\right] \tag{5}$$

Equations (3)–(5) show that $H_\epsilon(X,t)$ is harmonic only for the trivial case where $\omega_1 = \omega_2$, i.e., $U_{2x} = U_{1x}$ (we recall that the wavelength λ of sinusoidal surfaces is assumed to be the same on each surface).

3 Flow Factors Definition

As shown in [9], the unit flow averaged over the spatial period λ can be expressed through a macroscopic Reynolds equation:

$$\nabla \cdot \mathbf{q} = 0$$
$$\langle \mathbf{q} \rangle = -\frac{h_m^3}{12\mu}\phi \cdot \nabla\langle p\rangle + \frac{\langle h\rangle}{2}(\mathbf{U}_2 + \mathbf{U}_1) + \frac{\sigma}{2}\phi_s \cdot (\mathbf{U}_1 - \mathbf{U}_2) \tag{6}$$

Where, in the case of mono-dimensional surface roughness, flow factor tensors ϕ, and ϕ_s are diagonal and given by:

$$\phi = \begin{pmatrix} \phi_x & 0 \\ 0 & \phi_y \end{pmatrix} = \begin{pmatrix} \dfrac{1}{h_m^3\langle h^{-3}\rangle} & 0 \\ 0 & \dfrac{\langle h^3\rangle}{h_m^3} \end{pmatrix}, \tag{7}$$

$$\phi_s = \begin{pmatrix} \phi_{sx} & 0 \\ 0 & \phi_{sy} \end{pmatrix} = \begin{pmatrix} \dfrac{1}{\sigma\langle h^{-3}\rangle}\left\langle \dfrac{\tilde{h}_1 + \tilde{h}_2}{h^3}\right\rangle h_m & 0 \\ 0 & 0 \end{pmatrix} \tag{8}$$

While the averaged shear takes the form:

$$\langle \tau \rangle = \frac{\mu}{2}(\phi_f \pm \phi_{fs}) \cdot (\mathbf{U}_2 - \mathbf{U}_1) \pm \frac{h_m}{2}\phi_{fp} \cdot \nabla\langle p\rangle \tag{9}$$

With diagonal shear flow factors of the form:

$$\phi_f = \phi_f \mathbf{I} = h_m\langle h^{-1}\rangle \mathbf{I}$$
$$\phi_{fs} = \begin{pmatrix} 3h_m\left[\left\langle \dfrac{\tilde{h}_1 + \tilde{h}_2}{h^3}\right\rangle \dfrac{\langle h^{-2}\rangle}{\langle h^{-3}\rangle} - \left\langle \dfrac{\tilde{h}_1 + \tilde{h}_2}{h^2}\right\rangle\right] & 0 \\ 0 & 0 \end{pmatrix} \tag{10}$$

where $\mathbf{I}$ is the identity tensor and

$$\phi_{fp} = \begin{pmatrix} \phi_{fpx} & 0 \\ 0 & \phi_{fpy} \end{pmatrix} = \begin{pmatrix} \dfrac{\langle h^{-2}\rangle}{h_m\langle h^{-3}\rangle} & 0 \\ 0 & \dfrac{\langle h\rangle}{h_m} = 1 \end{pmatrix} \tag{11}$$

In these equations $\tilde{h}_i$ is the height variation of surface $i = 1,2$ around its mean plane, i.e., $h_i = \langle h_i\rangle + \tilde{h}_i$. $\langle h_i\rangle$ denotes the superficial surface average of h_i as defined in [9] and (12). Obviously, $\langle \tilde{h}_i\rangle = h_{io}$.

As pointed out in [9], Eqs. (6)–(11) are in complete agreement with the Patir and Cheng approach in this special case where the off-diagonal coefficient of the flow factor tensors are equal to zero. Being non-dimensional, the flow factors can be more appropriately expressed using dimensionless quantities H_ϵ, $\tilde{H}_{1\epsilon}$, and $\tilde{H}_{2\epsilon}$ (note that $H_\epsilon = 1 + \tilde{H}_{2\epsilon} - \tilde{H}_{1\epsilon}$). The expressions are similar to the above tensorial expressions, changing h and $\tilde{h}_i$ by H_ϵ, $\tilde{H}_{i\epsilon}$, for $i = 1,2$ respectively, and the composite r.m.s roughness σ by its following dimensionless counterpart $\Sigma = \sigma/h_m$ (which is a function of ϵ). As all geometric quantities are spatially periodic, of period λ in the x direction, and independent of y, the superficial average $\langle \psi \rangle$ of any function ψ can be expressed in terms of the dimensionless coordinate X as

$$\langle \psi(X,t)\rangle = \frac{1}{2\pi}\int_0^{2\pi} \psi(X,t)\,dX \tag{12}$$

The derivation of flow factors involves evaluating ''Sommerfeld'' integrals described in Appendix A. These integrals are defined if and only if $C_\epsilon(t) < 1$. It can be easily shown that this condition is verified for $\epsilon > 0$ (non-contact condition). This leads to express the flow factors as

$$\phi_x(t)=\frac{2(1-C_\epsilon(t)^2)^{5/2}}{(2+C_\epsilon(t)^2)} \quad \phi_y(t)=1+\frac{3}{2}C_\epsilon(t)^2$$

$$\phi_{sx}(t)=\frac{3\sqrt{2}(A_\epsilon^2-B_\epsilon^2)}{(2+C_\epsilon(t)^2)\sqrt{A_\epsilon^2+B_\epsilon^2}} \tag{13}$$

$$\phi_f(t)=\frac{1}{\sqrt{1-C_\epsilon(t)^2}} \quad \phi_{fsx}(t)=\frac{3(A_\epsilon^2-B_\epsilon^2)}{(2+C_\epsilon(t)^2)\sqrt{1-C_\epsilon(t)^2}}$$

$$\phi_{fpx}(t)=\frac{2(1-C_\epsilon(t)^2)}{(2+C_\epsilon(t)^2)}$$

Expressions (13) show that flow factors depend on: (1) both surfaces amplitudes A_ϵ and B_ϵ (2) time through the resulting amplitude $C_\epsilon(t)$ which is a periodic function of period $T=\lambda/(U_{2x}-U_{1x})$.

Thus, in general, the above flow factors are time periodic. It can be also seen that the flow factors ϕ_x, ϕ_y, ϕ_f, ϕ_{fp} are always positive, while the sign of the flow factors ϕ_s, ϕ_{fs} depends on the difference between surfaces amplitude.

At this stage, it is interesting to clearly distinguish two types of situation depending on the inter-correlation between the top and bottom surfaces. The intercorrelation function can be defined here as

$$C_{12}(l,t)=\frac{1}{\lambda}\int_0^\lambda (h_1(x,t)-\langle h_1(x,t)\rangle)(h_2(x+l,t)-\langle h_2(x,t)\rangle)dx \tag{14}$$

which leads to

$$C_{12}(l,t)=\sigma_1\sigma_2\cos\left(\frac{2\pi}{\lambda}(U_{2x}-U_{1x})t-\frac{2\pi l}{\lambda}+\varphi_1-\varphi_2\right) \tag{15}$$

Hence, the two aforementioned types of situations can be described as:

1. The case where there is no correlation between the two surfaces ($C_{12}(l,t)=0$). In this case one can consider that one of the two surfaces is smooth (for instance the top surface, $\sigma_2=0$), taking advantage on the surfaces roughness decorrelation. Then, in the referential frame of the moving rough surface, there is a permanent contact point in the limit $\epsilon=0$. Flow factors obtained in (13) become time independent. It is interesting to note that, in this case, the flow factors (as given by Eqs. (7), (8), and (9)) can be expressed in terms of spatial averages involving only the local aperture h (since here $\tilde{h}_2=0$ and $h=\langle h\rangle-\tilde{h}_1$):

$$\Phi_{sx}=\frac{1}{\sigma}\left(\langle h\rangle-\frac{\langle h^{-2}\rangle}{\langle h^{-3}\rangle}\right) \quad \Phi_{fsx}=3h_m\left(\left\langle h^{-1}-\frac{\langle h^{-2}\rangle^2}{\langle h^{-3}\rangle}\right\rangle\right) \tag{16}$$

   where the symbol Φ is used here (instead of ϕ) for clearly stressing that the above equations are valid only for the smooth/rough case and do not apply to the rough/rough case. For this first case, the spatial average performed above is sufficient to determine the average behavior, for which $C_\epsilon(t)=C_\epsilon=A_\epsilon$.
2. The case where there is a correlation between the upper and lower surfaces ($C_{12}(l,t)\neq 0$). Such correlation occurs naturally from elasto-plastic deformation during rolling process (see for example [10]). Here, we examine the case where both surfaces are rough ($A_\epsilon\neq 0$ and $B_\epsilon\neq 0$) leading to a sinusoidal inter-correlation function (15). As can be seen from Eq. (15), the two surfaces are perfectly correlated when they are in phase and perfectly uncorrelated when out of phase. On the contrary to the first case, contact is intermittent in the limit $\epsilon=0$. The relative motion of the two surfaces induces time variations of the local apertures and slopes. Under these circumstances, a time average must follow the spatial average for obtaining the average behaviors (that also could be obtained by ensemble averaging over all relative positions of two surfaces in the x direction). This is consistent with the fact that the time average of the inter-correlation function of Eq. (15) is zero.

Therefore, these two types of situation are associated with two types of averaging. The first one, i.e., the spatial averaging, is classical, see for instance [2,20,21] and references therein. The second type—i.e., spatio-temporal average—has not been considered to our knowledge, for flow factors computation. Discarding the spatio-temporal flow factor dependence is equivalent to choose a surface inter-correlation function equal to zero. Time averaging aspect of the problem has been, however, pointed out by Elrod [22].

4 Flow Factors Computation

4.1 Smooth-Rough Stationary Case. One of the two surfaces is smooth. Let us assume that this is the top surface, i.e., $b=B_\epsilon=0$, then $C_\epsilon=A_\epsilon$ and flow factors trivially reads from (13)

$$\phi_x=\frac{2(1-A_\epsilon^2)^{5/2}}{(2+A_\epsilon^2)} \quad \phi_y=1+\frac{3}{2}A_\epsilon^2 \quad \phi_{sx}=\frac{3\sqrt{2}A_\epsilon}{(2+A_\epsilon^2)}$$

$$\phi_f=\frac{1}{\sqrt{1-A_\epsilon^2}} \quad \phi_{fsx}=\frac{3A_\epsilon^2}{(2+A_\epsilon^2)\sqrt{1-A_\epsilon^2}} \quad \phi_{fpx}=\frac{2(1-A_\epsilon^2)}{(2+A_\epsilon^2)} \tag{17}$$

One first notes that these flow factors have the expected behaviors for large gaps between surfaces, i.e., ϕ_x, ϕ_y, ϕ_f, $\phi_{fpx}\to 1$ and ϕ_{sx}, $\phi_{fsx}\to 0$ (since $A_\epsilon\to 0$ when $\epsilon\to\infty$). Let us now consider their behaviors near contact, i.e., when $\epsilon\to 0$. According to the definition of A_ϵ (Eq. (1)), $\lim_{\epsilon\to 0}A_\epsilon=1-\epsilon/\sqrt{2}$. This leads to the following flow factors behaviors near contact, when $\epsilon\to 0$

$$\phi_x\to\frac{2}{3}(\sqrt{2}\epsilon)^{5/2} \quad \phi_y\to\frac{5}{2}-\frac{3}{\sqrt{2}}\epsilon \quad \phi_{sx}\to\sqrt{2}-\epsilon$$

$$\phi_f\to(\sqrt{2}\epsilon)^{-1/2} \quad \phi_{fsx}\to(\sqrt{2}\epsilon)^{-1/2} \quad \phi_{fpx}\to\frac{2\sqrt{2}}{3}\epsilon \tag{18}$$

As shown in Appendix B, these behaviors (except that of ϕ_y) can be obtained from the flow-factors definition itself using saddle point method, avoiding their explicit computation (17). Noting that $\langle h\rangle=a+\delta$ ($\delta=\epsilon\sigma$) and $\sigma=a/\sqrt{2}$, one obtains in terms of average unit flow when $\epsilon\to 0$

$$\langle q_x^\delta\rangle\to U_{1x}a+U_{2x}\delta-\frac{2\sqrt{2a}}{9\mu}\delta^{5/2}\frac{\partial\langle p\rangle}{\partial x}$$

$$\langle q_y^\delta\rangle\to\frac{U_{1y}+U_{2y}}{2}(a+\delta)-\frac{a^3}{12\mu}\left(\frac{5}{2}-3\frac{\delta}{a}\right)\frac{\partial\langle p\rangle}{\partial y} \tag{19}$$

From Eq. (19), it is interesting to note that the average Couette flow near contact in the x direction is made up of two contributions. The first one is the flow induced by the roughness corresponding to a fluid volume of mean thickness a transported at velocity U_{1x}. The second one is the flow induced by the top smooth surface carrying a small fluid volume of mean thickness δ at velocity U_{2x}. It is expected that the Poiseuille contribution to flow in the x direction, cancels out as the minimum aperture δ goes to zero, for obvious geometrical reasons. The 5/2 exponent dependence reflects the specific parabolic structure of the aperture field near contact, and can be obtained from simple saddle point argument (Appendix B). This behavior is generic for symmetrical aperture around the minimum in the x direction but will be different for non symmetrical ones. Flux in the y direction is simply that expected from a plane geometry. Let us now turn to the macroscopic shear:

$$\langle \tau_x^\delta(h_2)\rangle \to \mu(U_{2x}-U_{1x})\frac{1}{\sqrt{2a}}\delta^{-1/2}+\frac{2}{3}\delta\frac{\partial\langle p\rangle}{\partial x}$$

$$\langle \tau_x^\delta(h_1)\rangle \to -\frac{2}{3}\delta\frac{\partial\langle p\rangle}{\partial x}$$

$$\langle \tau_y^\delta(h_2)\rangle \to \mu(U_{2y}-U_{1y})\frac{1}{\sqrt{2a}}\delta^{-1/2}+\frac{a}{2}\frac{\partial\langle p\rangle}{\partial y} \qquad (20)$$

$$\langle \tau_y^\delta(h_1)\rangle \to \mu(U_{2y}-U_{1y})\frac{1}{\sqrt{2a}}\delta^{-1/2}-\frac{a}{2}\frac{\partial\langle p\rangle}{\partial y}$$

As expected, the main macroscopic shear comes from the Couette contribution. The obtained behaviors display a rather drastic divergence as the minimum aperture δ decreases. Here again, the $-1/2$ exponent is geometry dependent, related to the aperture symmetry around the contact point. It is worth noting that the y direction shows a symmetrical shear behavior (i.e., same behavior on surfaces 1 and 2), while on the x direction the shear is fully asymmetric: the flat surface experiences a major shear, while the sinusoidal one is almost not sheared at all. This is nothing but a lubrication effect of the sinusoidal surface in the vicinity of which a fluid layer moving at velocity U_{1x} annihilates the Couette shear.

4.2 Rough-Rough Unstationary Case. In this case, $A_\epsilon \neq 0$ and $B_\epsilon \neq 0$. Time averaging (13) over one period T is not straightforward owing to elliptic integrals of the first kind (K_1) and third kind (K_3) for Couette shear stress flow factors (see Appendix A). The final expressions read

$$\phi_x=\frac{4(1-(B_\epsilon-A_\epsilon)^2)^{5/2}}{\pi(2+(B_\epsilon-A_\epsilon)^2)}W(k^2,p^2) \qquad \phi_y=1+\frac{3}{2}(A_\epsilon^2+B_\epsilon^2)$$

$$\phi_{sx}=\frac{3\sqrt{2}(A_\epsilon^2-B_\epsilon^2)}{\sqrt{(A_\epsilon^2+B_\epsilon^2)(2+(B_\epsilon-A_\epsilon)^2)(2+(B_\epsilon+A_\epsilon)^2)}}$$

$$\phi_f=\frac{2}{\pi\sqrt{1-(B_\epsilon-A_\epsilon)^2}}K_1(k^2) \qquad (21)$$

$$\phi_{fsx}=\frac{6(A_\epsilon^2-B_\epsilon^2)}{\pi(2+(B_\epsilon-A_\epsilon)^2)\sqrt{1-(B_\epsilon-A_\epsilon)^2}}K_3(k^2,p^2)$$

$$\phi_{fpx}=\frac{6}{\sqrt{(2+(B_\epsilon-A_\epsilon)^2)(2+(B_\epsilon+A_\epsilon)^2)}}-2$$

where W is a definite and positive integral defined by

$$W(k^2,p^2)=\int_0^{\pi/2}\frac{(1-k^2\sin^2 v)^{5/2}dv}{(1+p^2\sin^2 v)},$$

$$k^2=\frac{4A_\epsilon B_\epsilon}{1-(B_\epsilon-A_\epsilon)^2}, \quad p^2=\frac{4A_\epsilon B_\epsilon}{2+(B_\epsilon-A_\epsilon)^2}$$

These results show that the flow factors ϕ_x, ϕ_y, and ϕ_{fpx}, associated with the average pressure gradient are always positive as represented in Figs. 3 and 4. The fluid can flow both in the direction perpendicular to streaks (i.e., along x) and in the direction parallel to streaks (i.e., along y) for the contact is only intermittent. As before, the shear stress flow factors ϕ_{sx} and ϕ_{fsx} depend on the difference between the surface amplitudes. It can be shown that the elliptic integrals of first kind $K_1(k^2)$ and third kind $K_3(k^2,p^2)$ diverge when the two surfaces are near contact, i.e., when $\epsilon\to 0$ and $k^2\to 1-\epsilon\sigma/2(1/a+1/b)$. As a result the flow factors behave asymptotically as $\epsilon\to 0$

$$\phi_x\to\frac{32}{\pi}\frac{(ab)^{3/2}}{(a+b)^3}\left\{p\left(1+\frac{1}{p^2}\right)^2\arctan(p)-\frac{5}{6}-\frac{1}{p^2}\right\}$$

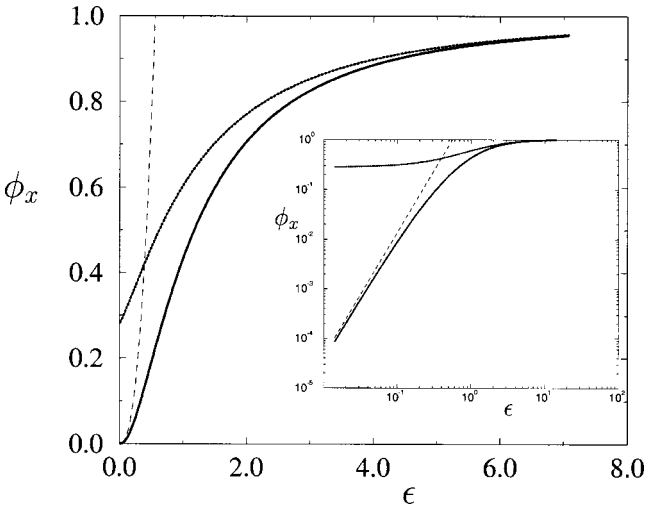

Fig. 3 Comparison of pressure flow factors ϕ_x calculated for stationary case (smooth/rough, solid line) and unstationary one (rough/rough, dotted line). The dashed line corresponds to the saddle point estimate near contact for the smooth/rough case. The inset shows the log-log plot of ϕ_x near contact with same conventions.

$$\phi_y\to 1+\frac{3}{2}\left(\frac{a^2+b^2}{(a+b)^2}\right)$$

$$\phi_{sx}\to\frac{\sqrt{6}(a^2-b^2)}{\sqrt{(a^2+b^2)[2(a+b)^2+(a-b)^2]}}$$

$$\phi_f\to-\frac{(b+a)}{2\pi\sqrt{ab}}\ln\left[\epsilon\frac{\sigma}{32}\left(\frac{1}{a}+\frac{1}{b}\right)\right] \qquad (22)$$

$$\phi_{fsx}\to-\frac{(a-b)}{2\pi\sqrt{ab}}\ln\left[\epsilon\frac{\sigma}{2^5}\left(\frac{1}{a}+\frac{1}{b}\right)\right]$$

$$\phi_{fpx}\to\frac{2\sqrt{3}(a+b)}{\sqrt{[2(a+b)^2+(a-b)^2]}}-2$$

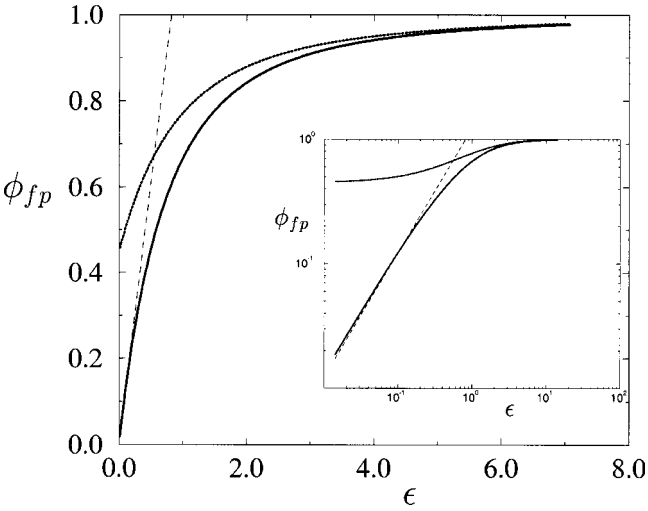

Fig. 4 Comparison of shear stress flow factors ϕ_{fpx} calculated for the stationary case (smooth/rough, solid line) and the unstationary one (rough/rough, dotted line). Same conventions as Fig. 3 have been used.

These results display a drastic difference from the stationary case (18). First as already observed on results (21), flow factors ϕ_x and ϕ_{fpx} converge to some positive constant which depends on the surfaces amplitude in a non trivial way, on the contrary to (18) where they tends to zero. These result simply indicate that even in the contact limit the aperture instationarity is a sufficient mechanism to produce flow and shear through pressure gradient in both x and y direction. Secondly, shear flow factors ϕ_f and ϕ_{fsx} diverge in the vicinity of contact, as observed in (18). Nevertheless, this divergence is quantitatively very different, being algebraic in (18) and logarithmic in (22). Such behavior can not be predicted using a saddle point approximation due to his non algebraic nature. It is nevertheless a result specific to the chosen geometry.

As a result, the average shear stress on each surfaces in the x direction, which is given, in the $\epsilon \to 0$ limit by

$$\begin{aligned}\langle \tau_x^{\delta}(h_2)\rangle \to \mu \frac{(U_{1x}-U_{2x})}{\pi(a+b)} \sqrt{\frac{a}{b}} \ln\left[\frac{\delta}{2^5}\left(\frac{1}{a}+\frac{1}{b}\right)\right] \\ + \frac{(a+b)}{2}\phi_{fpx}\frac{\partial\langle p\rangle}{\partial x} \\ \langle \tau_x^{\delta}(h_1)\rangle \to \mu \frac{(U_{1x}-U_{2x})}{\pi(a+b)} \sqrt{\frac{a}{b}} \ln\left[\frac{\delta}{2^5}\left(\frac{1}{a}+\frac{1}{b}\right)\right] \\ - \frac{(a+b)}{2}\phi_{fpx}\frac{\partial\langle p\rangle}{\partial x}\end{aligned} \tag{23}$$

also diverges logarithmically. Nevertheless, on the contrary to previous results (20) the Couette contribution to the shear in the x direction is now symmetrical on both surfaces, reflecting the geometry symmetry.

Regarding the average shear stress in the y direction, its behavior when $\epsilon \to 0$ reads

$$\langle \tau_y^{\delta}(h_2)\rangle \to \mu \frac{(U_{1y}-U_{2y})}{\pi(a+b)} \sqrt{\frac{b}{a}} \ln\left[\frac{\delta}{2^5}\left(\frac{1}{a}+\frac{1}{b}\right)\right] + \frac{(a+b)}{2}\frac{\partial\langle p\rangle}{\partial y} \tag{24}$$

$$\langle \tau_y^{\delta}(h_1)\rangle \to \mu \frac{(U_{1y}-U_{2y})}{\pi(a+b)} \sqrt{\frac{a}{b}} \ln\left[\frac{\delta}{2^5}\left(\frac{1}{a}+\frac{1}{b}\right)\right] - \frac{(a+b)}{2}\frac{\partial\langle p\rangle}{\partial y}$$

5 Discussion

The previously computed flow factors are sketched in Figs. 3–7 in order to investigate the composite roughness approximation in the context of sinusoidal surfaces. The flow factors displayed in these figures have been carefully compared with a direct numerical integration of expression Eqs. (7)–(11). Such numerical integration is in full agreement with the analytical results presented in the previous section. Both smooth/rough and rough/rough configuration are chosen with the same composite roughness leading to a rough surface amplitude $\sqrt{2}a$ in the smooth/rough case and $a=b$ in the rough/rough one.

For this particular choice, the Couette flow factors of the unstationary case are equal to zero ($\phi_{sx}=0$ and $\phi_{fsx}=0$). The asymptotic behaviors near contact deduced from the saddle point approximation (Appendix B) are also represented. These figures illustrate the following points:

- As shown in Figs. 3 and 4, the‘‘Poiseuille’’ flow factors ϕ_x and ϕ_{fpx} tend to zero near contact in the stationary case (smooth/rough), because, in this limit, contact permanently clogs the flow. Then, the fluid cannot migrate from one valley to the another whatever the pressure gradient is in the x direction. It is interesting to observe the quality and range of validity of the saddle point approximation in the close contact region shown in the insets of Figs. 3 and 4. This domain gives the region for which macroscopic behavior is dominated by the local structure of the aperture field near contact. On the contrary, in the unstationary case (rough/rough), flow factors ϕ_x and ϕ_{fpx} tend towards non zero constants in the contact limit. A fluid flow in the x direction driven by an average pressure gradient is then possible owing to the intermittent nature of contact.
- The shear flow factor ϕ_{sx} depends on the difference between the standard deviations of each surface. Hence, it can be either positive or negative. Interestingly, ϕ_{sx} is zero at contact in the particular case where the surfaces are strictly identical (Fig. 5). Roughness contribution to mean flow in the x direction due to the surfaces relative sliding is then canceling out. We recall from (6) that the mean flow due to sliding in the x direction is made up of two components. The first one is the Couette mean flow $(U_{2x}+U_{1x})\langle h\rangle/2$. The second one, $(U_{1x}-U_{2x})\sigma\phi_s/2$, is associated with the additional drag due to roughness. In the stationary case (smooth/rough) when the top surface is fixed and the rough bottom one is moving at velocity U_{1x}, the net mean flow due to sliding is $U_{1x}\langle h\rangle$. This exactly corresponds to the volume of dragged valleys

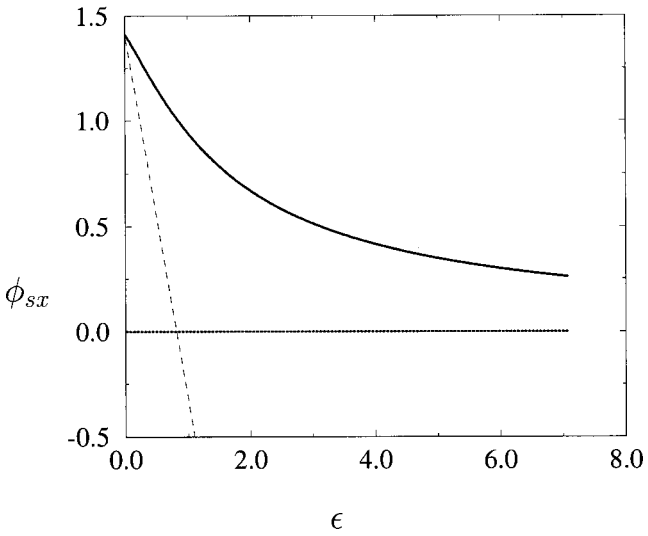

Fig. 5 Comparison of shear stress flow factors ϕ_{sx} calculated for the stationary case (smooth/rough, solid line) and the unstationary one (rough/rough, dotted line). Same conventions as Fig. 3 have been used.

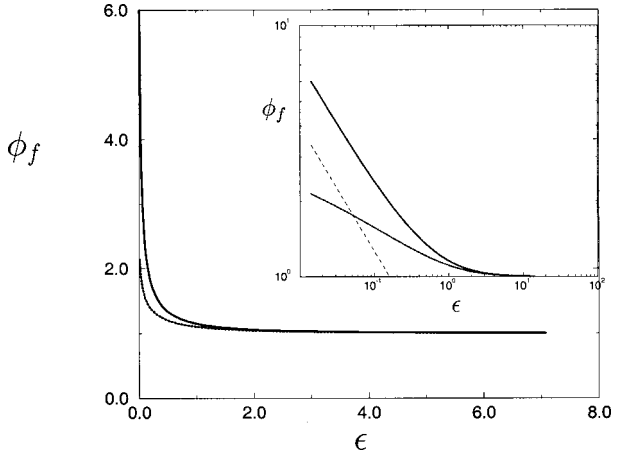

Fig. 6 Comparison of shear stress flow factors ϕ_f calculated for the stationary case (smooth/rough, solid line) and the unstationary one (rough/rough, dotted line). Same conventions as Fig. 3 have been used.

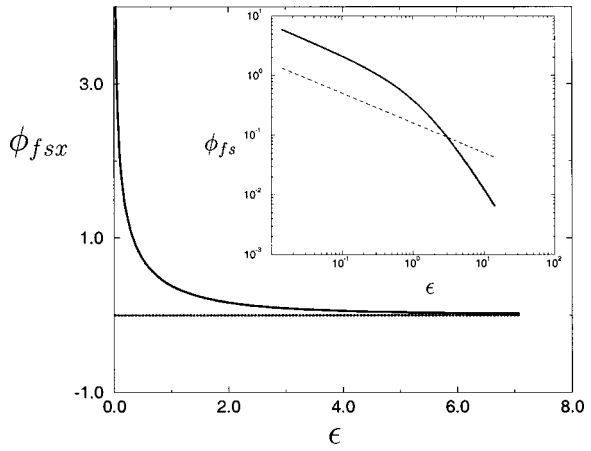

Fig. 7 Comparison of shear stress flow factors ϕ_{fsx} calculated for the stationary and the unstationary one. Same conventions as Fig. 3 have been used.

moving at the bottom surface velocity. This illustrates the coupled influence of geometry and kinematics on the mean flow due to sliding.

- In the stationary case, Couette shear stress flow factors ϕ_f and ϕ_{fsx} (Figs. 6 and 7) diverge as $\epsilon^{-1/2}$ near contact. ϕ_f is always positive whereas the sign of ϕ_{fsx} depends on the considered configuration. $\phi_{fsx}>0$ when the top surface is smooth and $\phi_{fsx}<0$ otherwise. This induces significant differences on the asymptotic behaviors of mean shear stress on each surface. We recall that the top surface experiences a mean shear stress proportional to $\phi_f+\phi_{fsx}$ while proportional to $\phi_f-\phi_{fsx}$ for the bottom one. Thus, in the stationary case, the rough surface experiences a mean shear stress diverging near contact as $\epsilon^{-1/2}$, while the mean shear stress tends to zero on the smooth surface. Obviously, this is only true in an average sense. Locally, the shear stress value can be very high. As previously noted, this singular behavior is related to the symmetry of the aperture geometry around the contact point.
- In the unstationary configuration, the flow factors ϕ_f and ϕ_{fsx} diverge logarithmically near contact (Figs. 6 and 7). The log-log plot in the inset displays the comparison between the algebraic and logarithmic divergence. ϕ_{fsx} depends however on the surface amplitude difference, and is equal to zero when surfaces amplitude are identical. The ''Couette'' mean shear stress experienced by each surface is positive and diverges logarithmically. Hence, here, the unsteadiness of the aperture field leads to a striking modification of shear stress behavior compared to the smooth-rough case. The local squeeze effects induced by the time evolution of the aperture field modify continuously the flow structure. As a result, pressure generation may occur in a divergent. This effect cannot occur in the steady smooth-rough case.

Lastly, when two rough surfaces are not intercorrelated, the flow factors ϕ_s and ϕ_{fs}, of each surface, can be expressed in terms of the corresponding flow factors of the smooth/rough case [2,5],

$$\phi_s=\frac{\sigma_1^2-\sigma_2^2}{\sigma^2}\Phi_s\left(\frac{h_m}{\sigma}\right) \qquad \phi_{fs}=\frac{\sigma_1^2-\sigma_2^2}{\sigma^2}\Phi_{fs}\left(\frac{h_m}{\sigma}\right) \tag{25}$$

where σ is the composite roughness as defined previously ($\sigma=\sqrt{\sigma_1^2+\sigma_2^2}$) and Φ_s, Φ_{fs} correspond to the smooth/rough case.

Clearly, these relations do no apply to the surfaces considered in the present paper (as can be easily checked analytically). In our case, the inter-correlation function is different from zero when both surfaces are rough and the composite roughness approximation associated with Eq. (25) is not valid.

Conclusions

Newtonian lubricant flow between two unidirectional wavy sinusoidal surfaces in sliding motion has been studied. Analytic expressions have been derived for flow factors describing the roughness impact on the macroscopic flow and shear. Two cases have been distinguished. In the first one, accounting for decorrelated surfaces, the aperture field is stationary and one of the two surfaces is smooth. Flows factor are then stationary and computed from simple spatial averaging. On the contrary, in the second case accounting for correlated surfaces (rough/rough case), the spatially averaged flow factors are time periodic. A temporal average leads to significant differences in the flow factor expressions. The obtained differences, can be regarded as resulting from the surface inter-correlation. Accordingly, the rough/rough situation investigated in the present paper is an example for which the composite roughness concept does not apply.

It is clearly expected that the observed drastic inter-correlation influence is enhanced by the deterministic nature of the chosen geometry as well as the considered roughness one-dimensional character. Nevertheless, for one-dimensional anisotropic surfaces, averaged stochastic geometries will share common features with our analysis.

Acknowledgments

This work was supported by the Research project contract (CPR) ''Mise en forme des matériaux: Contact outil-métal-lubrifiant'' between CNRS (SCA), Irsid (Usinor Group), Péchiney center de recherche de Voreppe, Paris Sud Orsay University (LMS), Collège de France (PMC), ECL (LTDS), INPT(IMFT), INSA de Lyon (LMC), ENSMP(CEMEF). The authors thank P. Montmitonnet for his remarks and suggestions.

Nomenclature

a, b	=	bottom surface and top surface amplitudes
A_ϵ	=	a/h_m
B_ϵ	=	b/h_m
$C_{12}(l,t)$	=	inter-correlation function between the two surfaces
$h(x,t)$	=	aperture field between the two surfaces
$\tilde{h}_i$	=	spatial fluctuation of the surface i
$h_m=h_{2o}-h_{1o}=a+b+\delta$	=	distance between surfaces mean plane which coincides with the mean distance between the two surfaces
$\langle h_i\rangle=h_{io}$	=	mean plane of surface i with $i=1,2$
H_ϵ	=	h/h_m
$\mathbf{I}$	=	identity tensor
k^2	=	$4A_\epsilon B_\epsilon/1-(B_\epsilon-A_\epsilon)^2$
K_1	=	elliptic integral of the first kind
K_3	=	elliptic integral of the third kind
$\mathbf{q}$	=	unit flow
$\mathbf{q}^\delta$	=	unit flow near contact
p^2	=	$4A_\epsilon B_\epsilon/2+(B_\epsilon-A_\epsilon)^2$
t	=	time
t_0	=	initial time
$T=\lambda/U_{2x}-U_{1x}$	=	time period
$\mathbf{U}_i$	=	surface velocity
x	=	coordinate perpendicular to the streak's direction
X	=	$2\pi x/\lambda$
y	=	coordinate parallel to the streak's direction
ϵ	=	δ/σ
δ	=	minimum local aperture

ϕ_i = phase of surface i at $t=t_0$

ϕ, ϕ_{fp} = Poiseuille flow factors tensors

ϕ_s, ϕ_f, ϕ_{fs} = Couette flow factors tensors

$\Phi_{sx}=\phi_{sx}$ = when surface 2 is smooth

$\Phi_{fsx}=\phi_{fsx}$ = when surface 2 is smooth

λ = wave length of sinusoidal surface

μ = fluid dynamic viscosity

$\sigma_1=\sqrt{a^2/2}$, $\sigma_2=\sqrt{b^2/2}$ = bottom surface, and top surface r.m.s roughness

$\sigma=\sqrt{\sigma_1^2+\sigma_2^2}$ = composite r.m.s roughness

$\tilde{\Sigma}$ = σ/h_m

τ = macroscopic tangential shear stress

τ^{δ} = macroscopic tangential shear stress near contact

$\langle\ \rangle$ = spatial average

Appendix A

Derivation of Eq. (3). Starting from Eq. (2),

$$H_\epsilon(X,t)=1+B_\epsilon\sin(X-\omega_2 t+\varphi_2)-A_\epsilon\sin(X-\omega_1 t+\varphi_1)$$

$H_\epsilon(X,t)$ can be expressed in terms of $\sin(X)$ and $\cos(X)$ as

$$H_\epsilon(X,t)=1+\sin(X)[B_\epsilon\cos\Phi_2-A_\epsilon\cos\Phi_1]+\cos(X)[B_\epsilon\sin\Phi_2-A_\epsilon\sin\Phi_1]$$

where $\Phi_i=-\omega_i\cdot t+\varphi_i$ $(i=1,2)$.

Then, defining the angle θ by

$$\tan\theta=\frac{B_\epsilon\sin\Phi_2-A_\epsilon\sin\Phi_1}{B_\epsilon\cos\Phi_2-A_\epsilon\cos\Phi_1}$$

allows one to express $H_\epsilon(X,t)$ as

$$H_\epsilon(X,t)=1+\frac{[B_\epsilon\cos\Phi_2-A_\epsilon\cos\Phi_1]}{\cos\theta}\{\sin X\cos\theta+\cos X\sin\theta\}$$

which gives

$$H_\epsilon(X,t)=1+\frac{[B_\epsilon\cos\Phi_2-A_\epsilon\cos\Phi_1]}{\cos\theta}\sin(X+\theta)$$

As $\cos^2\theta=1/(1+\tan^2\theta)$ one finally obtains

$$H_\epsilon(X,t)=1+\sqrt{A_\epsilon^2+B_\epsilon^2-2A_\epsilon B_\epsilon\cos[\Phi_2-\Phi_1]}\sin(X+\theta)$$

Sommerfeld Integral. As can be seen from Eqs. (7)–(11), the computation of flow factors necessitate the evaluation of the spatial averages $\langle H_\epsilon^3\rangle$, $\langle H_\epsilon^{-n}\rangle$, $n=2,3$, and $\langle(\tilde{H}_{1\epsilon}+\tilde{H}_{2\epsilon})/H_\epsilon^n\rangle$, $n=2,3$.

These averages reads,

$$\langle H_\epsilon^3\rangle=\frac{1}{2\pi}\int_0^{2\pi}(1+C_\epsilon(t)\sin(x+\theta_\epsilon(t))^3dx,$$

$$\langle H_\epsilon^{-n}\rangle=\frac{1}{2\pi}\int_0^{2\pi}\frac{1}{(1+C_\epsilon(t)\sin(x+\theta_\epsilon(t))^n}dx,$$

$$\left\langle\frac{\tilde{H}_{1\epsilon}+\tilde{H}_{2\epsilon}}{H_\epsilon^n}\right\rangle=\frac{1}{2\pi}\int_0^{2\pi}\frac{B_\epsilon\sin(x+\Phi_2)+A_\epsilon\sin(x+\Phi_1)}{(1+C_\epsilon(t)\sin(x+\theta_\epsilon(t))^n}.$$

Recalling that

$$C_\epsilon(t)=\sqrt{A_\epsilon^2+B_\epsilon^2-2A_\epsilon B_\epsilon\cos[(\omega_1-\omega_2)t+\varphi_2-\varphi_1]}$$

The evaluation of the first integral is trivial. The second and third integrals are a little more difficult. They can be expressed in terms of integrals of the form

$$S_{(m,n)}=\frac{1}{2\pi}\int_0^{2\pi}\frac{\cos^m\chi}{(1+C\cos\chi)^n}d\chi$$

These integrals (referred to as Sommerfeld integrals, see for instance [17]) can be evaluated analytically. The most useful formulas for our problem are the cases where m can take integer values 0 or 1 and $n=1,2,3$.

$$S_{(0,1)}=\frac{1}{\sqrt{1-C^2}}\quad S_{(0,2)}=\frac{1}{(1-C^2)^{3/2}}\quad S_{(0,3)}=\frac{2+C^2}{2(1-C^2)^{5/2}}$$

$$S_{(1,2)}=\frac{-C}{(1-C^2)^{3/2}}\quad S_{(1,3)}=\frac{-3C}{2(1-C^2)^{5/2}}$$

This leads to the expressions of flow factors given by Eq. (11). One can refer to [23] for more details

Elliptic Integrals. Let us first consider the definition of Elliptic integral of the first kind:

$$K_1(k^2)=\int_0^{\pi/2}\frac{dv}{\sqrt{1-k^2\sin^2 v}}=\frac{\pi}{2}F\left(\frac{1}{2};\frac{1}{2};1;k^2\right)$$

where F is the hyper-geometric function as described in [23]. In general, this integral must be evaluated numerically (see [24]). Again, an analytical evaluation can be performed near contact (i.e., when $k^2\to1$). This yields

$$\lim_{k^2\to1}K_1(k^2)=-\frac{1}{2}\ln\left(\frac{1-k^2}{2^4}\right)$$

Let us now turn to Elliptic integral of the third kind:

$$K_3(k^2,p^2)=\int_0^{\pi/2}\frac{dv}{(1+p^2\sin^2 v)\sqrt{1-k^2\sin^2 v}}$$

Again, in the general case, this integral must be evaluated numerically, [24].

Its asymptotic evaluation when $k^2\to1$ can be derived from that of $K_1(k^2)$ [23] since

$$\lim_{k^2\to1}K_3(k^2,p^2)=\frac{1}{1+p^2}\lim_{k^2\to1}K_1(k^2)$$

Appendix B

Saddle Point Estimate of Flow Factors Near Contact. Let us first turn our attention to the stationary case. The evaluation of flow factors (except ϕ_y, ϕ_{sy}, ϕ_{fsy}, and ϕ_{fpy} which are trivial ones) involves integrals of the form $\langle h^{-n}\rangle=1/\lambda\int h^{-n}dx$. Near contact, i.e., when $\epsilon\to0$., these integrals are dominated by the contribution associated with the lowest values of h. For this reason, it seems quite reasonable to seek an estimate of these integrals by the saddle point method [25]. Noting $f=h^{-n}$, this amounts to estimating $\langle f\rangle$ as $\sqrt{2\pi}/\lambda f(0)^{3/2}/\sqrt{-f''(0)}$ (in a coordinate system where $h=\epsilon$ at $x=0$). With $h=\epsilon+2a(1-\cos(2\pi/\lambda x))$, this leads to the following estimates as $\epsilon\to0$:

$$\phi_x\to\sqrt{3}\sqrt{2\pi}\epsilon^{5/2}\quad\phi_{sx}\to\sqrt{2}\left(1-\frac{\sqrt{3}}{\sqrt{2}}\epsilon\right)$$

$$\phi_f\to\frac{1}{\sqrt{2\pi}}\epsilon^{-1/2}\quad\phi_{fsx}\to\frac{3(2-\sqrt{3})}{2\sqrt{2\pi}}\epsilon^{-1/2}\quad\phi_{fpx}\to\sqrt{\frac{3}{2}}\epsilon$$

Scalings with ϵ are in full agreement with the results of the direct calculus (18). The prefactors are correctly estimated for ϕ_x, ϕ_{sx}, ϕ_{fpx} while not accurate for ϕ_f and ϕ_{fsx}. Such approximation can be applied to the unstationary case, but fails. The direct computation provides the explanation, as logarithmic divergence are beyond the scope of this rough estimate.

References

[1] Patir, N., and Cheng, H., 1978, ''An Average Flow Model for Determining Effects of Three-Dimensional Roughness on Partial Hydrodynamic Lubrication,'' ASME J. Lubr. Technol., **100**, p. 12.

[2] Patir, N., and Cheng, H., 1979, ''Application of Average Flow Model to Lubrication Between Rough Sliding Surfaces,'' ASME J. Lubr. Technol., **101**, p. 220.

[3] Christensen, H., 1970, ''Stochastic Models for Hydrodynamics Lubrication of Rough Surfaces,'' Int. J. of Mech. Eng., **104**, p. 1022.

[4] Chow, L., and Cheng, H., 1976, ''The Effect of Surface Roughness on the Average Film Thickness Between Lubricated Rollers,'' ASME J. Lubr. Technol., **98**, p. 117.

[5] Tripp, J., 1983, ''Surface Roughness Effects in Hydrodynamic Lubrication: The Flow Factor Method,'' ASME J. Lubr. Technol., **105**, p. 458.

[6] Bayada, G., and Chambat, M., 1988, ''New Models in the Theory of the Hydrodynamic Lubrication of Rough Surfaces,'' ASME J. Tribol., **110**, p. 402.

[7] Bayada, G., and Faure, J., 1989, ''A Double Scale Analysis Approach of the Reynolds Roughness. Comments and Application to the Journal Bearing,'' ASME J. Tribol., **111**, p. 323.

[8] Whitaker, S., 1999, *The Method of Volume Averaging*, Kluwer Academic Publishers.

[9] Letalleur, N., Prat, M., and Plouraboué, F., 2002, ''Averaged Reynolds Equation for Flow Between Rough Surfaces in Sliding Motion,'' Trans. Por. Med., in press.

[10] Plouraboué, F., and Boehm, M., 1999, ''Multiscale Roughness Transfer in Cold Metal Rolling,'' Tribol. Int., **32**, p. 45.

[11] Bhushan, B., and Blackman, G., 1991, ''Atomic Force Microscopy of Magnetic Rigid Disks and Sliders and Its Applications to Tribology,'' ASME J. Tribol., **113**, p. 452.

[12] Mahumdar, A., and Tien, C. L., 1990, ''Fractal Characterization and Simulation of Rough Surfaces,'' Wear, **160**, p. 313.

[13] Yang, M., and Talke, F., 1993, ''Surface Roughness Investigation of Magnetic Recording Disk Using STM and Profilometry Measurements,'' Wear, **170**, p. 15.

[14] Michell, A., 1950, *Lubrication—Its Principle and Practice*, Blakie and Son, London and Glasgow.

[15] Burton, R., 1963, ''Effects of Two-Dimensional, Sinusoidal Roughness on the Load Support Characteristics of a Lubricant Film,'' ASME J. Basic Eng., **84**, p. 197.

[16] Fantino, B., 1973, *Influence des défauts de forme dans la lubrification hydrodynamique*, Thèse de l'Université Claude Bernard de Lyon.

[17] Hamrock, B., 1994, *Fundamentals of Fluid Film Lubrication*, McGraw-Hill.

[18] Hemmat, M., and Borhan, A., 1995, ''Creeping Flow Through Sinusoidally Constricted Capillaries,'' Phys. Fluids, **7**, pp. 2111—2121.

[19] Plouraboué, F., Prat, M., and Letalleur, N., 2001, ''Sliding Lubricated Anisotropic Rough Surfaces,'' Phys. Rev. E, **64**(1), pp. 011202-1.

[20] Peeken, H., Knoll, G., Rienacker, A., Lang, J., and Schonen, R., 1997, ''On the Numerical Determination of Flow Factors,'' ASME J. Tribol., **119**, p. 259.

[21] Knoll, G., Rienacker, A., Lagemann, V., and Lechtape-Gruter, R., 1998, ''Effect of Contact Deformation on Flow Factors,'' ASME J. Tribol., **120**, p. 140.

[22] Elrod, H., 1979, ''A General Theory for Laminar Lubrication With Reynolds Roughness,'' ASME J. Lubr. Technol., **101**, p. 8.

[23] Abramowitz, M., and Stegun, I., 1972, *Handbook of Mathematical Functions*, Dover, New York.

[24] Press., W., Teukolsky, S., and Flannery, W. V. B., 1995, *Numerical Recipes in Fortran*, Cambridge University Press.

[25] Hinch, E., 1991, *Perturbation Methods*, Cambridge University Press.